Published in final edited form as:
IEEE Trans Biomed Eng. 2011 April ; 58(4): 868–875. doi:10.1109/TBME.2010.2097598.

Three-dimensional Imaging of Ventricular Activation and Electrograms from Intracavitary Recordings

Chenguang Liu[Member, IEEE], **Paul A. Iaizzo[Member, IEEE]**, and **Bin He[Fellow, IEEE]**
University of Minnesota, Minneapolis, MN 55455 USA (binhe@umn.edu)

Abstract

Three-dimensional mapping of the ventricular activation is of importance to better understand the mechanisms and facilitate management of ventricular arrhythmia. The goal of the present study was to develop and evaluate a three-dimensional cardiac electrical imaging (3DCEI) approach for imaging myocardial electrical activation from the intracavitary electrograms and heart-torso geometry information over the 3-dimensional (3D) volume of the heart. The 3DCEI was evaluated in a swine model undergoing intracavitary non-contact mapping (NCM). Each animal's pre-operative MRI data were acquired to construct the heart-torso model. NCM was performed with the Ensite® 3000 system during acute ventricular pacing. Subsequent 3DCEI analyses were performed on the measured intracavitary electrograms. The estimated initial sites (ISs) were compared to the precise pacing locations, and the estimated activation sequences (ASs) and electrograms (EGs) were compared to those recorded by the NCM system over the endocardial surface. In total, 6 ventricular sites from 2 pigs were paced. The averaged localization error of IS was 6.7 ± 2.6 mm. The endocardial ASs and EGs as a subset of the estimated 3-dimensional solutions were consistent with those reconstructed from the NCM system. The present results demonstrate that the intracavitary-recording-based 3DCEI approach can well localize the sites of initiation and can obtain physiologically reasonable activation sequences as well as electrograms in an in vivo setting; under control/paced conditions. The present study suggests the feasibility of tomographic imaging of 3D ventricular activation and 3D electrograms from intracavitary recordings.

Index Terms

Activation imaging; Cardiac electrical imaging; Intracavitary recordings; Intramural potential mapping

I. INTRODUCTION

The electrical activity associated with ventricular arrhythmias is often distributed over the three-dimensional ventricular myocardium and evolves over time. Thus spatio-temporal mapping of electrophysiological sources accompanying arrhythmias has led to significant advancement in our understanding of the mechanisms of arrhythmias [1] and in aiding clinical management of arrhythmias, e. g. guiding catheter ablation [2] and guiding the implantation for cardiac resynchronization therapy [3]. Noninvasive body surface electrocardiographic recordings have been used to estimate epicardial potentials and derived electrophysiological properties [4], the activation sequence over the epicardial and

Correspondence to: Bin He.

endocardial surfaces [5], and the activation sequence throughout the 3-dimensional (3D) myocardium [6]–[8].

To date, spatio-temporal mapping approaches used in clinical medicine are mainly based on the endocardial surface approach. The CARTO® (Biosense Webster, Belgium) system conducts direct electro-anotomic mapping over the endocardial surface by the sequential acquisition of electrograms (EGs) to construct electrical activity over the endocardial surface [9]–[10]. While being widely used in the cardiac electrophysiology labs, the CARTO® system is limited in mapping nonsustained arrhythmias due to the requirement of multiple-beat recordings. Instantaneous intracavitary recordings have been used to solve the inverse problem in order to obtain the endocardial mapping results [11]–[12], and the Ensite® system (St Jude Medical, Inc.) is widely used to estimate the endocardial potentials from the intracavitary potential maps (ICPMs) recorded by a multi-electrode array (MEA) from a balloon catheter [13].

Though successful, these surface mapping approaches (direct or indirect) are limited in their ability to characterize subsurface activities, e.g. intramural delay [14]. 3D mapping of cardiac activities could not only be a powerful tool for research on the mechanisms of arrhythmias [1], [15]–[17], but could also guide the clinical management of cardiac arrhythmias in a more efficient way. Specifically, localization of the initial site of activation implies direct clinical benefits for the management of arrhythmias caused by focal initiation, such as focal ventricular tachycardia and adenosine insensitive microreentry [18]. The localization of focal initiations has the potential of guiding ablative procedures. Secondly, mapping global ventricular activation sequence can provide an outlook of the cardiac activity as well as local details. Lastly, the estimated intramural electrograms could replace invasive intraoperative sensors to disclose the intrinsic characteristics of the heart excitation, in both spatial and temporal domains.

In order to address this issue, we have proposed the three-dimensional cardiac electrical imaging (3DCEI) approach, a novel functional imaging method using intracavitary recordings, to reconstruct electrical activation in 3D myocardium from endocardium to epicardium [19]. In the present study, we report for the first time experimental data to image 3D activation sequence from intracavitary recordings. We further propose a novel approach to estimate intramural electrograms, which, to our knowledge, represents the first report of indirectly mapping transmural potentials from the intracavitary recordings or any other non-contact recordings. Animal studies were conducted to experimentally evaluate the performance of this newly proposed 3D functional tomographic imaging technique. Ventricular pacing at different locations was conducted to simulate focal arrhythmogenic activities. The 3D locations of the initiation sites, the resultant activation sequences and the intramural electrograms were estimated by employing the 3DCEI approach and the results were evaluated with the aid of magnetic resonance imaging (MRI) and the Ensite® system.

II. METHODS

A. Swine model and data collection

Control pigs (n = 2, weight = 85.8 kg and 83.2 kg, respectively) were employed in the present study. For each animal, pre-operative magnetic resonance imaging (MRI; ECG gated to end diastole with breath held) data were acquired approximately 5–7 days before the *in vivo* mapping experiment to obtain the anatomical geometry information. Short-axis scanning from neck to abdomen with a slice thickness of 3 mm was performed. The surgical preparation of these animals for hemodynamic and electrical monitoring has been previously reported [20]. During the mapping studies, each animal was anesthetized with fentanyl infused at 0.75 mcg/kg/min; all were intubated and mechanically ventilated with 65% air

and 35% O_2 to maintain a $PaCO_2$ of 40 ± 2 mmHg. The intracavitary potential mapping was conducted by employing the EnSite® 3000 noncontact mapping (NCM) system (St Jude Medical, Inc., St. Paul, MN) which consists of a 64-multielectrode array (MEA) mounted on a 9-Fr balloon catheter. The balloon catheter and a standard EP catheter were put into the left ventricle (LV). The 3D location of the roving catheter's electrode relative to the fixed, known position of the expanded balloon was obtained by the NCM system. 3D reconstructions of the LV chamber's endocardial geometry were created by moving the roving catheter around the chamber, while the system accumulated anatomic reference points.

For each animal, active-fixation pacing leads were screwed into the right ventricular apex (RVA) and the RV septum (RVS) (Model 3830, Medtronic, Inc., USA) to deliver intramural pacing. Endocardial surface pacing was accomplished by a quadripolar EP catheter in the LV at the following areas: LV anterior (LVAn), LV middle lateral (LVML), LV lower lateral (LVLL) and LV apex (LVA). The 3D locations of the endocardial pacing sites were recorded on the reconstructed LV geometry acquired with the NCM system. ICPMs were recorded by the MEA when pacing was conducted. After the completion of the data collection procedure, the heart was removed and fixed in formalin with the intramural pacing leads remaining in place. These isolated hearts were again MRI scanned to record the precise locations of the RV pacing sites.

B. Forward problem and modeling

The schematic diagram of the ICPM-based 3DCEI approach is shown in Fig. 1. For each animal, a heart-torso volume conductor model was constructed based on the pre-operative MRI scans and prior known physiological knowledge. The segmentation of the MRI data was conducted in a commercial software package CURRY 5.0, where a set of MRI slices was imported and the geometry could be displayed on three planes: short axis, sagittal and coronal. Segmentation was then performed interactively on all of the three planes. The space between the epicardium and the endocardia was discretized into over 100,000 cellular units (spatial resolution of 1.5 mm) and a cellular-automaton heart-excitation model was constructed by assigning *a priori* physiological knowledge to the cardiac tissues which were made up by those cellular units. A universal waveform of the action potential [21] was assigned to every cellular unit in the ventricles, which starts with the very steep phase 0 and followed by the transient phase 1. Since only the activation of the heart was simulated and utilized in the present study, the diversity of phase 2 as well as phase 3 had little effect and so it was neglected in the present study. The other parameters of each cellular unit, such as cell type, conductivity tensors, etc., were assigned as well. Then the activation of the heart could be simulated based on cellular automaton to obtain the activation time at any ventricular location. Once the activation time τ at location k in the ventricles and the waveform of the trans-membrane action potential at k are known, the equivalent current density at time instant t at the location k can be calculated as follows,

$$j^k(t) = -\sigma_i \nabla V^k(\tau, t) \tag{1}$$

where σ_i is the intracellular conductivity tensor, V the transmembrane potential. Thus the equivalent current densities at thousands of uniformly distributed locations inside the myocardium were calculated representing the ventricular activities during activation. Based on the bidomain theory, the field potential ϕ can be calculated from those current sources employing the Poisson's equation [19],

$$\nabla \cdot [(\sigma_i + \sigma_e)\nabla\phi] = \nabla \cdot j \tag{2}$$

where σ_e is the extracellular conductivity tensor. Eq. (2) was numerically solved using the finite element method (FEM). By using variational principle and applying Galerkin method, Eq. (2) was eventually transformed into such a set of linear equations:

$$2S \cdot \phi = -G \tag{3}$$

where S is the stiffness matrix containing the information of the finite element (FE) model, G is the load matrix containing the information transformed from the equivalent current densities and ϕ is the vector of potentials at every node of the FE model. Since S is a large sparse matrix, Eq. (3) was solved with the preconditioned conjugate gradients method.

For applying FEM, a FE model was constructed based on the MR images and the NCM system's recording. The geometries of the torso and heart were obtained by segmenting the MR images, while the geometries and relative locations of the MEA and LV were recorded by the NCM system. In order to obtain the accurate location of the MEA in the heart-torso volume conductor, a registration procedure between the LV's endocardial surface extracted from the MR images and the corresponding surface recorded by the NCM system was performed.

The registration included two steps. First, initial transformation parameters were obtained by "landmark registration", during which 3 to 4 anatomical endocardial locations in the two sets of encocardial surfaces were manually fitted. Second, "surface registration" was performed. The two surfaces were registered by applying a multidimensional registration approach based on the Euclidean distance transform and the Marquardt-Levenberg optimization algorithm [22]. After the registration, the coordinates of the MEA were transformed to the coordinate system of the heart-torso volume conductor, based on which the torso-heart-catheter FE model was constructed. Theoretically, the electric potential at every node of the FE model can be calculated when the electrical source is known. The potentials at 64 nodes corresponding to the locations of the intracavitary electrodes on the MEA were extracted to constitute the ICPMs at a given time. Thus the forward relationship between the cardiac sources and the ICPMs was set up.

C. Inverse calculation

Based on the forward modeling described above, a heart-model-based estimation algorithm was optimized to derive the cardiac activation sequence from the raw ICPMs recorded by the MEA in the NCM system [19]. The parameters of the numerical heart model were initialized by using a preliminary classification system [23], and the corresponding ICPM was calculated by using FEM. The heart model's parameters were then iteratively adjusted in an attempt to minimize the dissimilarity between the measured and the heart-model-generated ICPMs. The details of the algorithm with which the locations of the initiation sites and the activation sequences were estimated were described in [19].

The estimation of the 3D potentials/electrograms throughout the ventricles was based on the estimated 3D activation sequence with the above approach. Once the estimated activation sequence had been obtained, the intramural potentials could be calculated by solving Eq. (2) using FEM.

In theory, the field potential at every node of the finite element model can be calculated, including the nodes inside the myocardium. To ensure the accuracy of the calculated intramural potentials, a fine source model was required. The entire ventricles were divided into around 6,000 small segments and the activity in each segment was represented by a

local equivalent current density. The FE model was also finer at the heart area than other areas to reduce the numerical error in the calculation of intramural potentials.

D. Evaluation of the imaging solutions in experiments

The performance of the 3DCEI approach was validated in terms of localization errors of the initiation sites of activation. The estimated activation sequences as well as electrograms (EGs) were analyzed and compared with those reconstructed by the endocardial NCM system over the endocardial surface.

The locations of the initiation sites of activation were estimated in the heart-excitation models which were obtained from the pre-operative MR images. The precise locations of LV pacing sites were recorded by the NCM system and were subsequently obtained in the heart-excitation model after the LV endocardial surface registration procedure described above. On the other hand, the precise locations of the RV pacing sites were obtained by locating the distal end of the pacing leads in the post-operative MR images of the isolated hearts (note that each heart was fixed in an end diastolic state). For the purpose of determining the precise 3D locations of the initiation sites in the resultant heart-excitation models, the surface registration procedure described above was performed between the isolated, fixed heart and the beating heart. After the registration, the precise locations of the initial activation sites in RV were determined in the heart-excitation model and could be directly compared with the estimated locations.

The mapped 3D ventricular activation sequences were evaluated by comparing with the results of the NCM system over the left ventricular endocardium. Though the reconstructed endocardial electrograms and activation sequence by the NCM system are not gold standards, those mapping results are still appreciable considering the broad clinical application. So the endocardial activation sequences were extracted from the 3DCEI solutions, and then projected from the endocardial surfaces of the heart models to the endocardial surfaces recorded by the NCM system for comparison. Similarly, the estimated electrograms were also evaluated by comparison to the output of the NCM system over the endocardial surface.

III. RESULTS

A. Localization of the initiation site of activation

Pacing studies were conducted in four LV and two RV pacing sites. Well captured beats corresponding to the pacing sites were picked up and analyzed, respectively. The locations of the initiation sites and the localization error (LE) for each pacing site are summarized in Table I. Over the four LV pacing sites, the averaged localization error was 5.3 mm. The averaged LE undergoing RV pacing was 9.5 mm, which might be due to farther distance from MEA to the pacing site. In summary, the averaged LE over all pacing sites was 6.7 ± 2.6 mm (mean ± standard deviation).

B. Estimation of the 3D activation sequence

The ICPM-based 3DCEI analysis was applied to those pacing data and the 3D activation sequences were functionally mapped. Fig. 2 depicts an example of the mapped activation sequence when the heart was paced from the RV septum. In Fig. 2, the activation wavefront initiated from the septum and propagated to LV and RV, respectively. The wavefront reached the LV endocardium (the breakthrough point is indicated with a green star) at the 9th ms after initiation of activation and finally died out at the LV free wall. Another local maximum of activation time located at the RV free wall. It has been shown that both surface information and transmural information were included in our results and were

straightforwardly illustrated. Physiologically reasonable activation sequences throughout the ventricles were obtained from all of the six pacing studies.

The endocardial activation sequences were then extracted from our 3D estimation results and compared with that of the NCM system. Since the NCM system's output regarding the endocardial activation sequence was a color-coded plot instead of quantitative data, qualitative comparison was made between the activation sequence estimated by 3DCEI and the NCM system's output. Fig. 3(a) depicts the extraction of the endocardial activation sequence from our 3D results and the comparison between the two sets of endocardial activation sequences when pig #1 was paced from the RV apex. In the 3D results shown in the first column, the estimated initial area of activation is located at the RV apex. The activation wavefront propagated across the ventricles and ended at the LV free wall. Regarding the extracted activation sequence on the LV endocardium, it was found that the mapping result by 3DCEI was consistent with the output of the NCM system for the general propagation pattern. The earliest endocardial activation site estimated by 3DCEI (indicated by number “1”) was located at the apical-septal area, very close to the pacing site; the corresponding area illustrated by the NCM system was on the left side of LV apex, which might have an acceptable bias. On the other hand, the late activation areas indicated by 3DCEI and the NCM system were quite consistent.

Fig. 3(b) depicts another example when pig #2 was paced from the LV apex. It was observed that 3DCEI and the NCM system nicely supported each other regarding the depolarization propagation, illustrating reasonable consistency between these two sets of results.

C. Estimation of intramural electrograms

Fig. 4 depicts an example of the reconstructed potentials and electrograms when the heart was paced from LV apex. Fig. 4(a) shows the distribution of transmural potentials illustrating propagation of excitation throughout the 3D ventricles. Corresponding to the depolarization, the interstitial potential of a myocardial site decreased dramatically when the propagation wavefront arrived. The evolvement of the depolarization wavefront throughout the 3D myocardium can be clearly observed from the series of isopotential maps over time in Fig. 4(a). The estimated series of 3D isopotential maps offered “virtual” electrograms should electrodes be placed intramurally. To evaluate the estimated EGs, ten different sites on the endocardial surface were selected from the 2,048 virtual endocardial sites exported from the NCM system. Since it has been reported that the accuracy of the exported EGs from the Ensite system is more reliable when the distance between the MEA and the endocardium is less than 40 mm [32], those ten sites were picked up from the endocardial area where the distance to the MEA was relatively small. The reconstructed EGs by 3DCEI at those sites were compared with the EGs reconstructed by the NCM system as shown in Fig. 4(c), where the consistency between the two sets of EGs was demonstrated by the averaged correlation coefficient (CC) of 0.73. The averaged CC of EGs at all virtual endocardial sites whose distances to the MEA were no more than 40 mm was 0.73, too. Although the imaging results were consistent in general pattern, some discrepancies were observed. There was a timing shift in waveform 6, and the EGs reconstructed by 3DCEI showed slower recovery from the negative peak in waveform 7, 8, 9 and 10. The possible reason for this discrepancy will be discussed in the Discussion section.

Fig. 5 depicts another example of the reconstructed EGs when the heart was paced from RV septum. The averaged correlation coefficient between the waveforms of EGs at 12 typical sites shown in Fig. 5(c) was 0.77. The averaged CC of EGs at all endocardial sites whose distances to the MEA were no more than 40 mm was 0.70. The animated high-resolution iso-potential maps of the entire activation procedure corresponding to all six pacing studies

can be seen in the supplementary video clips. Displaying the evolvement of the iso-potential maps during activation is equivalent to displaying the estimated intramural EGs at all virtual ventricular sites.

IV. DISCUSSION

Functional cardiac electrical imaging has shown great promises in mapping cardiac activation from body surface potential maps (BSPMs) [4]–[8], [24]–[30] or from endocardial approaches [11]–[13]. Most of the functional cardiac imaging or mapping has been focused on heart surface approaches, including epicardial potential imaging, heart surface activation imaging, or endocardial surface mapping. While 3D functional cardiac electrical imaging is desirable, it requires solving an ill-posed inverse problem to obtain intramural information.

He and co-workers have previously investigated the 3D cardiac activation imaging from BSPMs [6]–[8], [29]–[30]. Electrophysiological cardiac excitation can be simulated from the cell level to the whole heart [31], and in our heart-model-based imaging approach, a cellular-automaton heart model [23] is employed to incorporate prior knowledge about the cardiac electrophysiology. Recently, He et al further proposed the 3-dimensional cardiac electrical imaging (3DCEI) from intracavitary recordings, which are routinely made in a clinical setting [19]. Due to the vicinity of intracavitary sensors to the heart and the clinical use of MEA, the intracavitary potential maps (ICPMs) based 3DCEI may provide clinically important information guiding management of arrhythmias.

We report here a novel approach to estimate the intramural electrograms, and provides the first experimental evidence with regard to the feasibility of tomographic imaging of the 3D cardiac electrical activities including field potentials and activation sequence, from intracavitary noncontact measurements. This experimental study provides a carefully designed evaluation of these novel methods, either proposed in this work (intramural potential imaging) or previously proposed but without experimental evaluation [19]. The present promising experimental results indicate the good localization ability of the methods, and suggest the feasibility of the proposed methods in imaging activation sequence and intramural potentials by comparing with the known knowledge of cardiac electrophysiology and the corresponding output of the NCM system on the LV endocardium. Though the mapping results by the NCM system are not necessarily a gold standard and are limited on the endocardial surface, they have been widely used in clinical EP labs, thus representing an important comparison study. On the other hand, studies with the aid of direct three-dimensional mapping techniques, such as mapping with intramural needle electrodes, shall fully validate the 3DCEI approach in the future. The promising evaluation results in the present study suggest the potential of the novel 3DCEI technique to image 3D electrical activities from intracavitary recordings. Furthermore, the ICPM-based 3DCEI approach may take advantage of the short distance between the intracavitary recordings and the cardiac sources to reveal subtle cardiac events imperceptible from the body surface, and such studies are expected in the future

Localization of the initiation site of excitation and/or arrhythmogenic substrate is of importance for guiding catheter ablation. Efforts have been made to find the initiation sites of cardiac events on the heart surfaces by employing an inverse calculation [4], [13], [27]. Compared to those surface imaging approaches, the 3DCEI approach has the potential of providing comprehensive 3D information of functional anatomy, which is of importance for characterizing and localizing arrhythmias of sub-endocardial or intramural origins. In the present study, the successful localization of the initiation site induced by pacing suggests the

potential of localizing the initiation sites of focal ventricular tachycardia and/or other cardiac arrhythmias throughout the 3D myocardium.

An interesting phenomenon is that 3DCEI performed better when localizing the pacing sites in LV than in RV; that is, smaller localization error was observed when the pacing site was in LV. Corresponding to the pacing sites at LV lateral and LV apex in pig #2, the LE were 4.2 mm and 4.7 mm, respectively. On the other hand, the LE corresponding to the pacing site at RV apex in pig #1 was 10.8 mm. Due to the limited number of pacing sites in this pilot study, rigorous statistical analysis has not been performed. The difference in localization errors between LV and RV might be attributed to the fact that the balloon catheter was placed in the LV, and the assumption can be made that the smaller distance between the MEA and the pacing site in LV resulted in smaller localization error. A recent study also supported this notion that in the NCM system, if the imaged source is farther from the balloon catheter, the accuracy of the mapping results will decrease [32]. Such results are consistent with our understanding that signals generated by closer sources are better reflected in the recordings and therefore the sources could be more accurately reconstructed in an inverse approach. In future practical applications, the MEA should be put in the appropriate chamber to keep it relatively close to the region of interest. Nevertheless, even when the origin of activation is relatively far from the MEA, 3DCEI can still reconstruct reasonable mapping results which are fairly consistent with the output of the NCM system (see Fig. 3 (a) and Fig. 5).

Mapping the cardiac activation sequence is useful for revealing the underlying mechanism of arrhythmias and facilitating the subsequent treatment. Specifically, 3D activation sequence mapping provides a straightforward method to characterize the cardiac events originating from the subsurface substrates. The imaged 3D activation sequence by 3DCEI can provide detailed 3D information (see Fig. 2 and Fig. 3), which is especially useful for areas with thick myocardium, such as apical area and LV free wall. Considering that not all arrhythmogenic substrates are accessible from endocardium, the necessity of applying epicardial ablation needs to be determined in some cases. Accounting for its ability of providing global activation sequence, the 3DCEI approach may play an important role in detecting non-subendocardial arrhythmogenic substrates and selecting appropriate treatment options.

Direct intra-operative mapping can provide an important insight into the intrinsic characteristics of cardiac events [1], [16]–[17]. The unique information provided by intramural EGs can increase our understanding of the mechanisms of arrhythmic events and aiding clinical management of arrhythmias. In the present study, we reported the first effort of estimating the EG at any intramural site throughout the ventricles. Such estimated intramural EGs can be considered as an approximation of extracellular potentials, which would be recorded should one put a large number of electrodes within the ventricular volume. The 3D isopotential maps shown in Fig. 4 and Fig. 5 (and supplementary videos) reveal the ability of 3D potential mapping in providing spatiotemporal information regarding cardiac electrical activity, depicting that our technique can present 3D potentials in great detail. Most of the noninvasive or minimally-invasive mapping methods limit the results on the heart surface (endocardium, or epicardium, or both); the intra-operative mapping with needle electrodes can provide real 3D mapping results, but the procedure is inconvenient and the cardiac tissue has to be destroyed at some level. Compared to those mapping methods, the 3DCEI approach only needs minimally-invasive intracavitary recordings but can present 3D results transmurally like the intra-operative mapping.

The fiber structure and related anisotropic conductivity of the myocardium have effects on the spread of excitation and the morphology of intramural electrograms [33]. In the present

study, the anisotropic nature of the heart was not considered and the heart model used in 3DCEI approach was assumed to be isotropic, which might be responsible for the inconsistency of the EGs 7–10 shown in Figure 4. Incorporating anisotropy should benefit the accuracy of the inverse solutions and the reported localization error and estimation error may be further reduced if conductivity anisotropy is incorporated in the forward model. In this pilot study, we have reported the concepts and principles of the 3D intramural extracellular potential imaging, and the first experimental results of 3D intramural extracellular potential imaging and of the ICPM-based 3DCEI. In future investigations, conductivity anisotropy could be incorporated from information obtained by using diffusion tensor magnetic resonance imaging (DT-MRI) [34]. DT-MRI can detect the fiber orientation in the 3D space based on the phenomenon that water diffuses more rapidly in the direction aligned with the fibrous structure. The fiber orientation at any position of the heart could be obtained via a full magnetic resonance scan and so could be incorporated into the 3DCEI approach.

The number of animals (n=2) employed in the present pilot study is small. Nevertheless, the present pilot study for the first time reports the experimental evaluation of the ICPM-based 3DCEI. Furthermore, to our knowledge, the novel method with regard to three-dimensional imaging of intramural extracellular potentials has been for the first time proposed and then evaluated in animal experiments. In future studies, a larger population need to be used to thoroughly evaluate our approach.

A well-controlled pacing protocol has been employed, and the promising experimental results suggest that the intracavitary-based 3DCEI approach may enhance our ability to map focal ventricular arrhythmias. On the other hand, it is worthy of noting that the activation due to pacing is relatively simple. While beyond the scope of the present study, in order to tackle more complex cardiac events with the 3DCEI approach, the employed heart model need to be further refined by incorporating appropriate electrophysiological properties in future studies.

Supplementary Material

Refer to Web version on PubMed Central for supplementary material.

Acknowledgments

The authors would like to thank Dr. Cory Swingen, Dr. Nicholas Skadsberg, Dr. Sarah Ahlberg, Bill Gallagher and Dr. Christopher Wilke for technical assistance of the data acquisition, and Dr. Eric Voth from St. Jude Medical for technical assistance in converting the data format for Ensite system.

This work was supported in part by NIH R01HL080093, NSF CBET-0756331. Chenguang Liu was supported in part by a Doctoral Dissertation Fellowship from the Graduate School of the University of Minnesota.

REFERENCES

1. Attin M, Ideker RE, Pogwizd SM. Mechanistic insights into ventricular arrhythmias from mapping studies in humans. Heart Rhythm. 2008; vol. 5 Suppl(6):S53–S58. [PubMed: 18456203]
2. Zeppenfeld K, Schalij MJ, Bartelings MM, Tedrow UB, Koplan BA, Soejima K, Stevenson WG. Catheter ablation of ventricular tachycardia after repair of congenital heart disease: electroanatomic identification of the critical right ventricular isthmus. Circulation. 2007; vol. 116:2241–2252. [PubMed: 17967973]
3. Helm RH, Byrne M, Helm PA, Daya SK, Osman NF, Tunin R, Halperin HR, Berger RD, Kass DA, Lardo AC. Three-dimensional mapping of optimal left ventricular pacing site for cardiac resynchronization. Circulation. 2007; vol. 115:953–961. [PubMed: 17296857]

4. Ramanathan C, Ghanem RN, Jia P, Ryu K, Rudy Y. Noninvasive electrocardiographic imaging for cardiac electrophysiology and arrhythmia. Nature Medicine. 2004; vol. 10:422–428.
5. Berger T, Fischer G, Pfeifer B, Modre R, Hanser F, Trieb T, Roithinger FX, Stuehlinger M, Pachinger O, Tilg B, Hintringer F. Single-beat noninvasive imaging of cardiac electrophysiology of ventricular pre-excitation. J. Am. Coll. Cardiol. 2006; vol. 48:2045–2052. [PubMed: 17112994]
6. He B, Li G, Zhang X. Noninvasive three-dimensional activation time imaging of ventricular excitation by means of a heart-excitation model. Phys. Med. Bio. 2002; vol. 47:4063–4078. [PubMed: 12476982]
7. Zhang X, Ramachandra I, Liu Z, Muneer B, Pogwizd SM, He B. Noninvasive three-dimensional electrocardiographic imaging of ventricular activation sequence. Am. J. Physiol. Heart. Circ. Physiol. 2005; vol. 289:H2724–H2732. [PubMed: 16085677]
8. Liu C, Skadsberg N, Ahlberg S, Swingen C, Iaizzo PA, He B. Estimation of global ventricular activation sequences by noninvasive 3-dimensional electrical imaging: validation studies in a swine model during pacing. J. Cardiovasc. Electrophysiol. 2008; vol. 19:535–540. [PubMed: 18179521]
9. Ben-Haim SA, Osadchy D, Schuster I, Gepstein L, Hayam G, Josephson ME. Nonfluoroscopic, in vivo navigation and mapping technology. Nature Med. 1996; 2:1393–1395. [PubMed: 8946843]
10. Gepstein L, Hayam G, Ben-Haim SA. A novel method for nonfluoroscopic catheter-based electroanatomical mapping of the heart: in vitro and in vivo accuracy results. Circulation. 1997; vol. 95:1611–1622. [PubMed: 9118532]
11. Khoury DS, Taccardi B, Lux RL, Ershler PR, Rudy Y. Reconstruction of endocardial potentials and activation sequences from intracavitary probe measurements: localization of pacing sites and effects of myocardial structure. Circulation. 1995; vol. 91:845–863. [PubMed: 7828314]
12. Schilling RJ, Peters NS, Davies DW. Simultaneous endocardial mapping in the human left ventricle using a noncontact catheter: comparison of contact and reconstructed electrograms during sinus rhythm. Circulation. 1998; vol. 98:887–898. [PubMed: 9738644]
13. Gornick CC, Adler SW, Pederson B, Hauck J, Budd J, Schweitzer J. Validation of a new noncontact catheter system for electroanatomic mapping of left ventricular endocardium. Circulation. 1999; vol. 99:829–835. [PubMed: 9989971]
14. Avari JN, Rhee EK. Cardiac resynchronization therapy for pediatric heart failure. Heart Rhythm. 2008; vol. 5:1476–1478. [PubMed: 18672406]
15. Witkowski FX, Corr PB. An automated simultaneous transmural cardiac mapping system. Am. J. Physiol. 1984; vol. 247:H661–H668. [PubMed: 6496707]
16. Chung MK, Pogwizd SM, Miller DP, Cain ME. Three-dimensional mapping of the initiation of nonsustained ventricular tachycardia in the human heart. Circulation. 1997; vol. 95:2517–2527. [PubMed: 9184582]
17. Zhang S, Skinner JL, Sims AL, Rollins DL, Walcott GP, Smith WM, Ideker RE. Three-dimensional mapping of spontaneous ventricular arrhythmias in a canine thrombotic coronary occlusion model. J. Cardiovasc. Electrophysiol. 2000; vol. 11:762–772. [PubMed: 10921794]
18. Mittal S. "Focal" ventricular tachycardia: insights from catheter ablation. Heart Rhythm. 2008; vol. 5 Suppl(6):S64–S67. [PubMed: 18456205]
19. He B, Liu C, Zhang Y. Three-dimensional cardiac electrical imaging from intracavity recordings. IEEE Trans. Biomed. Eng. 2007; vol. 54:1454–1460. [PubMed: 17694866]
20. Laske TG, Skadsberg ND, Hill AJ, Klein GJ, Iaizzo PA. Excitation of the intrinsic conduction system through his and intraventricular septal pacing. Pacing Clin. Electrophysiol. 2006; vol. 29:397–405. [PubMed: 16650269]
21. Ohyu S, Okamoto Y, Kuriki S. Use of ventricular propagated excitation model in the magnetocardiographic inverse problem for reconstruction of electrophysiological properties. IEEE Trans. Biomed. Eng. 2002; vol. 49:509–519. [PubMed: 12046695]
22. Kozinska D, Tretiak OJ, Nissanov J, Ozturk C. Multidimensional alignment using the euclidean distance transform. Graphical Models and Image Processing. 1997; vol. 59:373–387.
23. Li G, He B. Localization of the site of origin of cardiac activation by means of a heart-model-based electrocardiographic imaging approach. IEEE Trans. Biomed. Eng. 2001; vol. 48:660–669. [PubMed: 11396596]

24. Barr RC, Ramsey M 3rd, Spach MS. Relating epicardial to body surface potential distributions by means of transfer coefficients based on geometry measurements. IEEE Trans. Biomed. Eng. 1977; vol. 24:1–11. [PubMed: 832882]

25. Greensite F, Huiskamp G. An improved method for estimating epicardial potentials from the body surface. IEEE Trans. Biomed. Eng. 1998; vol. 45:98–104. [PubMed: 9444844]

26. Oster HS, Taccardi B, Lux RL, Ershler PR, Rudy Y. Electrocardiographic imaging: Noninvasive characterization of intramural myocardial activation from inverse-reconstructed epicardial potentials and electrograms. Circulation. 1998; vol. 97:1496–1507. [PubMed: 9576431]

27. Tilg B, Fischer G, Modre R, Hanser F, Messnarz B, Schocke M, Kremser C, Berger T, Hintringer F, Roithinger FX. Model-based imaging of cardiac electrical excitation in humans. IEEE Trans. Med. Imaging. 2002; vol. 21:1031–1039. [PubMed: 12564871]

28. Cheng LK, Bodley JM, Pullan AJ. Comparison of potential- and activation-based formulations for the inverse problem of electrocardiology. IEEE Trans. Biomed. Eng. 2003; vol. 50:11–22. [PubMed: 12617520]

29. Liu Z, Liu C, He B. Noninvasive reconstruction of three-dimensional ventricular activation sequence from the inverse solution of distributed equivalent current density. IEEE Trans. Med. Imaging. 2006; vol. 25:1307–1318. [PubMed: 17024834]

30. Han C, Liu Z, Zhang X, Pogwizd SM, He B. Noninvasive three-dimensional cardiac activation imaging from body surface potential maps: a computational and experimental study on a rabbit model. IEEE Trans. Med. Imaging. 2008; vol. 27:1622–1630. [PubMed: 18955177]

31. Hunter PJ, Pullan AJ, Smaill BH. Modeling total heart function. Annu. Rev. Biomed. Eng. 2003; vol. 5:147–177. [PubMed: 14527312]

32. Abrams DJ, Earley MJ, Sporton SC, Kistler PM, Gatzoulis MA, Mullen MJ, Till JA, Cullen S, Walker F, Lowe MD, Deanfield JE, Schilling RJ. Comparison of noncontact and electroanatomic mapping to identify scar and arrhythmia late after the Fontan procedure. Circulation. 2007; vol. 115:1738–1746. [PubMed: 17372177]

33. Taccardi B, Macchi E, Lux RL, Ershler PR, Spaggiari S, Baruffi S, Vyhmeister Y. Effect of myocardial fiber direction on epicardial potentials. Circulation. 1994; vol. 90:3076–3090. [PubMed: 7994857]

34. Helm P, Beg MF, Miller MI, Winslow RL. Measuring and mapping cardiac fiber and laminar architecture using diffusion tensor MR imaging. Ann. N. Y. Acad. Sci. 2005; vol. 1047:296–307. [PubMed: 16093505]

Biographies

Chenguang Liu (S’05–M’10) received the B.S. and M.S. degrees in biomedical engineering from Tsinghua University, Beijing, China, in 2001 and 2003, respectively, and the Ph.D. degree in biomedical engineering from the University of Minnesota, Twin Cities, in 2010.

He is currently a Postdoctoral Associate at Department of Biomedical Engineering, University of Minnesota. His research interests include biological signal processing, system modeling, interventional electrophysiology, electrocardiography forward and inverse problem, and animal experimentation.

Paul Iaizzo (M’ 09) earned the PhD degree in Physiology, and is Professor of Surgery, Integrative Biology and Physiology, Anesthesiology, and Carlson School of Management at the University of Minnesota.

He currently heads the Visible Heart® Laboratory, where his main research focus is translational systems physiology and his research group has developed a unique isolated working large mammalian heart model.

Bin He (S'87–M'88–SM'97–F'04) received the BS degree (Highest Honors) in electrical engineering from Zhejiang University, Hangzhou, China, and the Ph.D. degree (Highest Honors) in bioelectrical engineering from Tokyo Institute of Technology, Japan.

He completed the Postdoctoral Fellowship in biomedical engineering from Harvard University– Massachusetts Institute of Technology, Cambridge, MA. He is currently a Distinguished McKnight University Professor and Professor of Biomedical Engineering at the University of Minnesota, Twin Cities, where he is also currently the Director of the Center for Neuroengineering.

He has pioneered the development of electric source imaging, and made significant contributions to functional neuroimaging, cardiac electrical tomography, brain–computer interface, and magnetoacoustic tomography. His research interests include neuroengineering, functional biomedical imaging, and bioelectromagnetism.

Prof. He is a Fellow of the American Institute for Medical and Biological Engineering, the Institute of Physics, and the International Society for Functional Source Imaging. He was the recipient of the National Science Foundation CAREER Award and the American Heart Association Established Investigator Award.

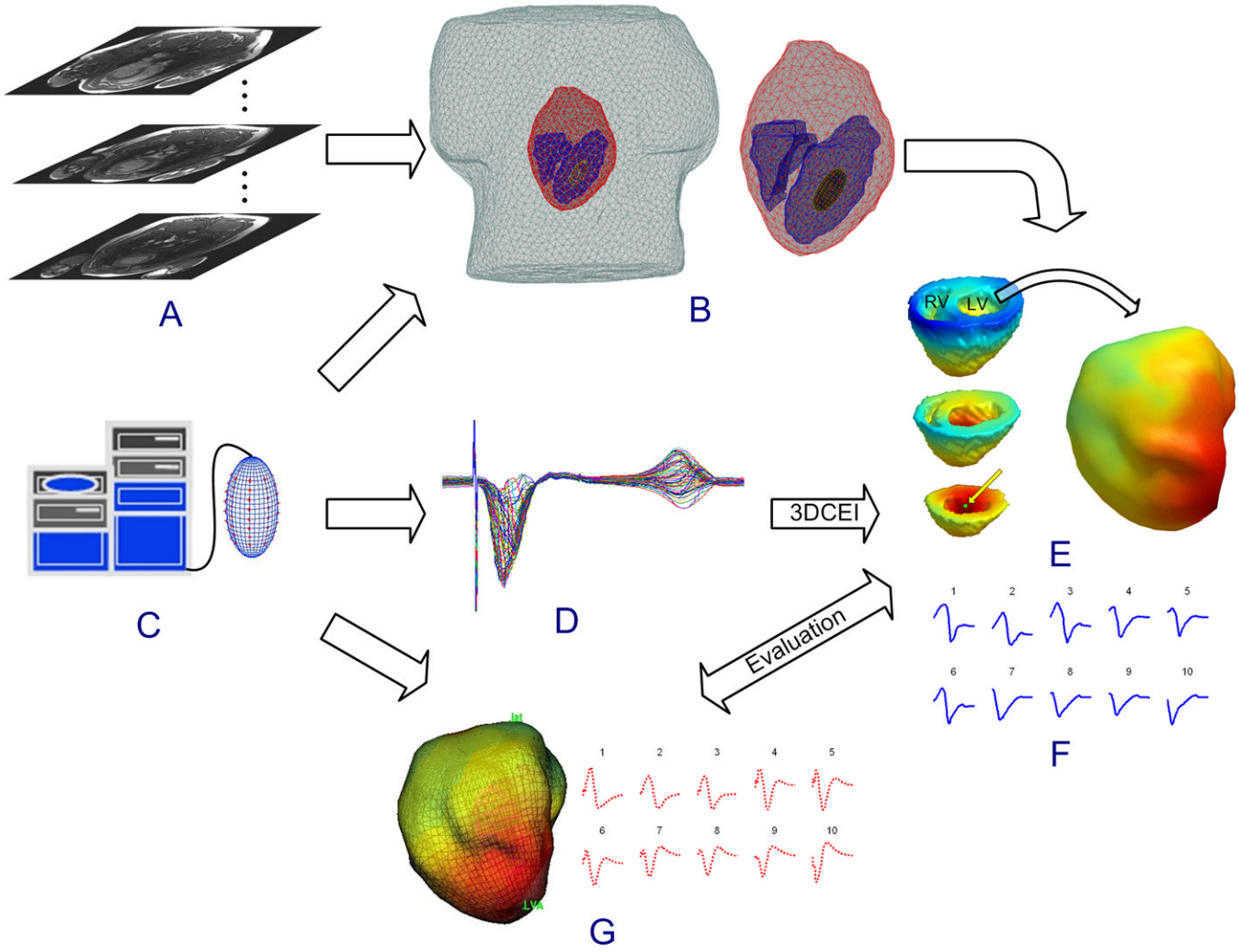

Fig. 1.

The schematic diagram of the ICPM-based three-dimensional electrical imaging approach. A: the MR images of the individual pig. B: the heart-torso model including the balloon catheter. C: the intracavitary mapping system. D: the butterfly plot of the intracavitary electrograms. E: the reconstructed activation sequence and the estimated initiation site by 3DCEI. F: the reconstructed electrograms by 3DCEI. G: the reconstructed cardiac activities by the intracavitary mapping system.

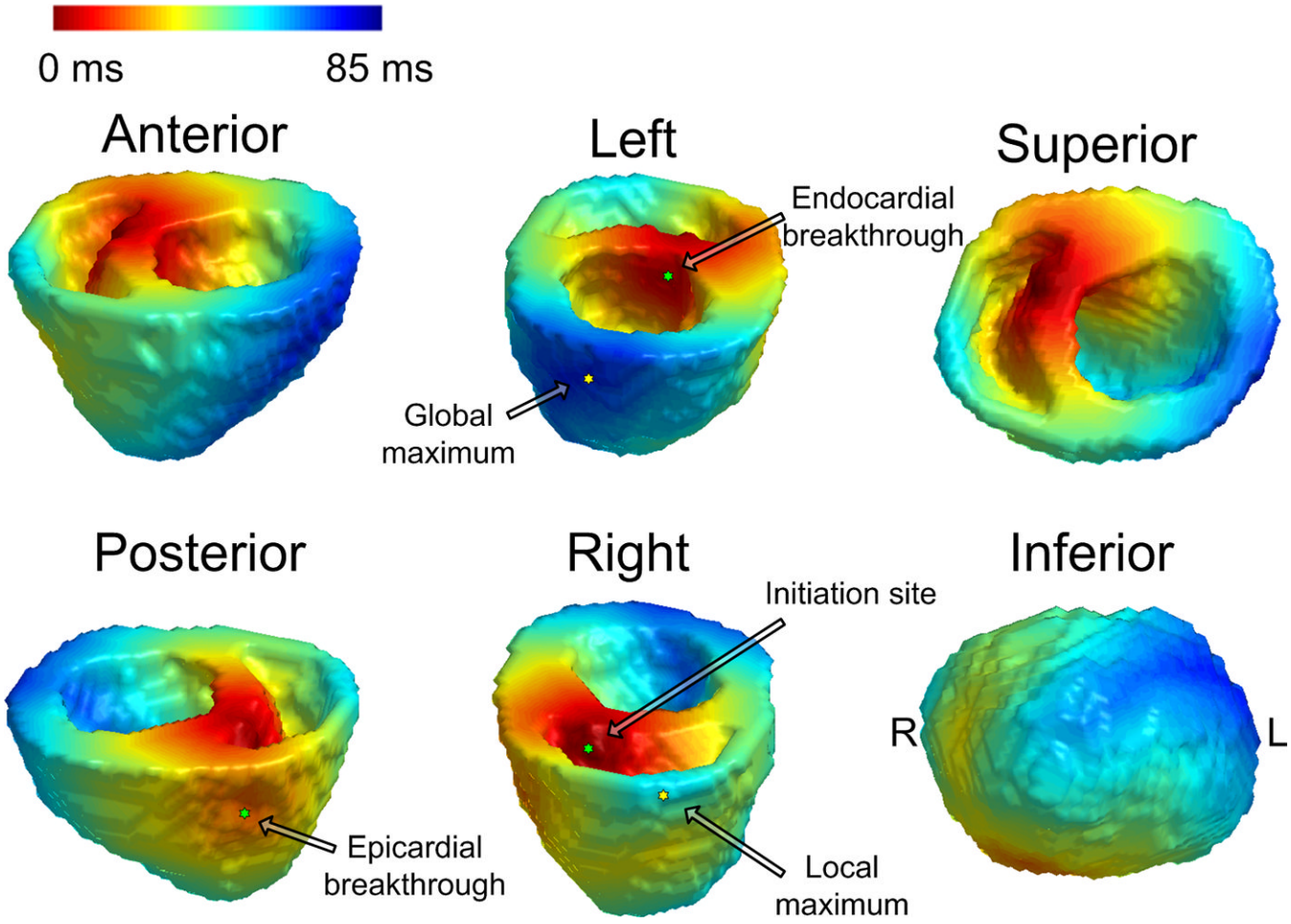

Fig. 2.

The imaged three-dimensional activation sequence when the heart was paced from the RV septum. The activation sequence is shown in six view angles. RED represents the earliest activated area and BLUE represents the latest activated area.

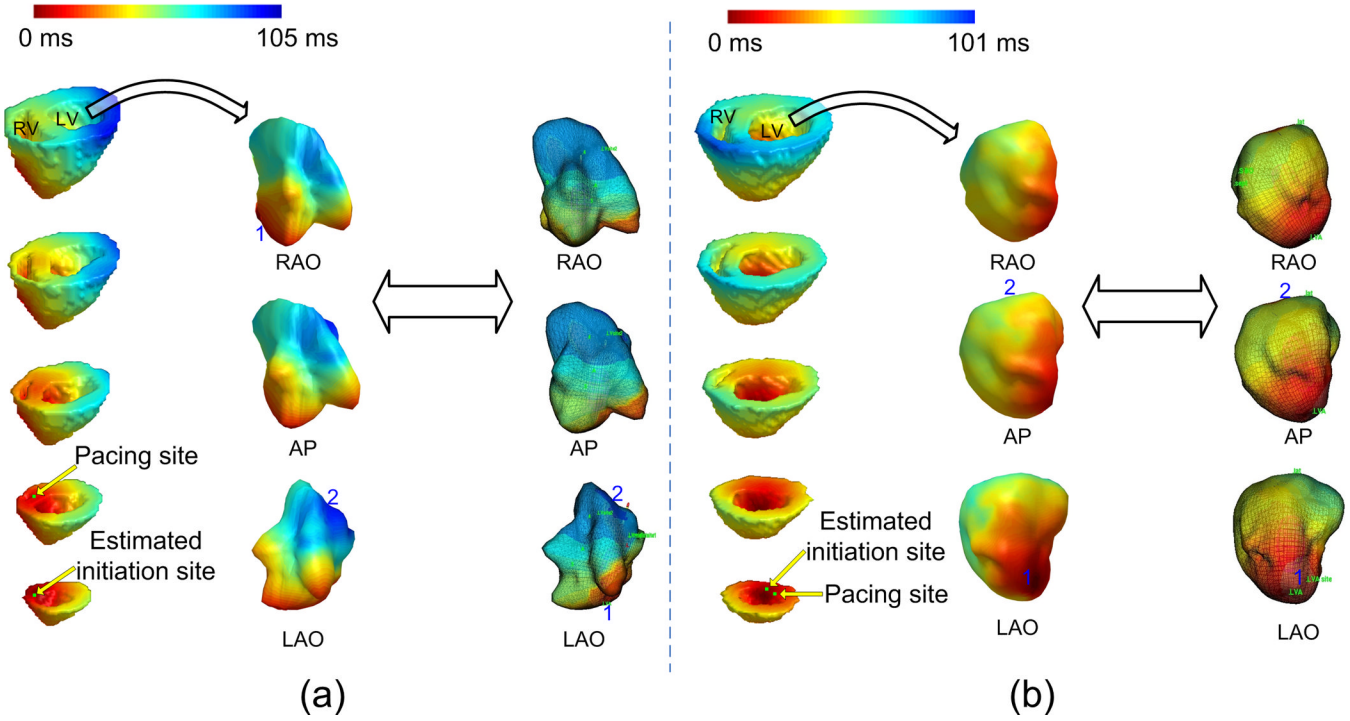

Fig. 3.

The evaluation of the estimated activation sequence when: (a) the pig #1 was paced from RV apex; (b) the pig #2 was paced from the LV apex. In each panel, the 3D activation sequence (AS) throughout the ventricles is shown in the left column. The precise location of the pacing site and the estimated location of the initiation site are indicated. The AS on the LV endocardial surface is extracted from the 3D solutions and shown in the middle column in 3 views: RAO, AP and LAO. The corresponding endocardial AS reconstructed by the intravitary noncontact mapping system is shown in the right column for comparison. The earliest activated site is indicated by the number “1” and the latest activated site is indicated by “2” on the figure.

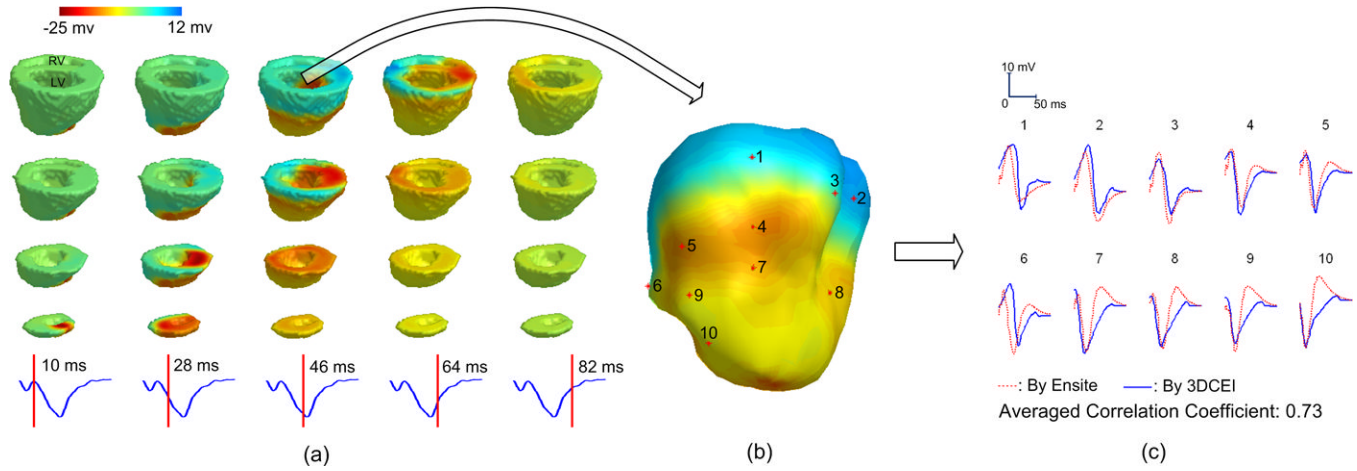

Fig. 4.

The evaluation of the estimated electrograms when the heart is paced from the LV apex. (a) The 3D potential maps throughout the ventricles. The potential maps are shown on different horizontal levels from base to apex (each column), and in time sequence. The time instant after pacing corresponding to each column is indicated on the lead II ECG waveform. (b) The extracted endocardial potential map at the 46th ms after pacing and the locations of selected 10 sites on the endocardial surface. (c) The comparison of the reconstructed electrograms between the NCM system and the 3DCEI approach at 10 endocardial sites. The locations of the 10 sites are indicated in panel (b).

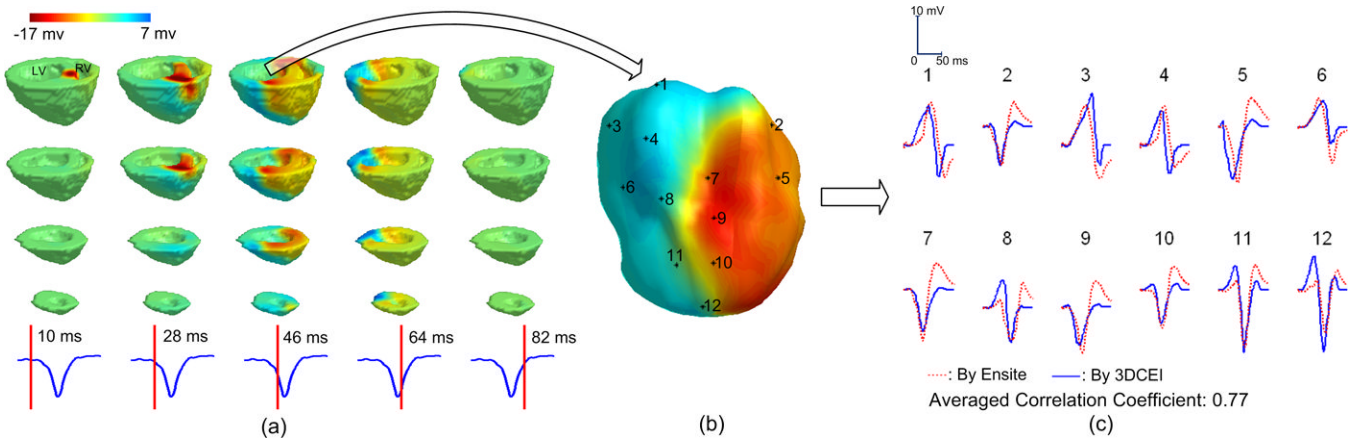

Fig. 5.

The evaluation of the estimated electrograms when the heart is paced from the RV septum. (a) The 3D potential maps throughout the ventricles. The potential maps are shown on different horizontal levels from base to apex (each column), and in time sequence. The time instant after pacing corresponding to each column is indicated on the lead II ECG waveform. (b) The extracted endocardial potential map at the 46th ms after pacing and the locations of selected 12 sites on the endocardial surface. (c) The comparison of the reconstructed electrograms between the NCM system and the 3DCEI approach at 12 endocardial sites. The locations of the 12 sites are indicated in panel (b).

TABLE I

Localization Error

Pig #	**1**	**1**	**2**	**2**	**2**	**2**
Pacing site	RVA	LVML	RVS	LVA	LVLL	LVAn
Localization error (mm)	10.8	7.6	8.1	4.7	4.2	4.5